Journal of the European Ceramic Society 20 (2000) 1895–1900

Load-dependence of Knoop hardness of Al_2O_3–TiC composites

Jianghong Gong *, Zhe Zhao, Zhenduo Guan, Hezhuo Miao

Department of Materials Science and Engineering, Tsinghua University, Beijing 100084, PR China

Received 27 November 1999; received in revised form 26 February 2000; accepted 12 March 2000

Abstract

Nine samples of Al_2O_3–30 wt.% TiC composites were prepared by hot-pressing the Al_2O_3 powder mixed with TiC particles. The average sizes of the TiC particles used for preparing the nine samples were different with each other. Knoop hardness measurements were conducted on these nine samples, respectively, in the indentation load range from 1.47 to 35.77 N. For each sample, the measured Knoop hardness decreases with the increasing indentation load. The classical Meyer's power law and an empirical equation proposed originally by Bückle were verified to be sufficiently suitable for describing the observed load-dependence of the measured hardness. Analysis based on Meyer's law can not provide any useful information about the cause of the observed ISE while true hardness values, which are load-independent, can be deduced from the Bückle's equation. It was found that the deduced true hardness increases with the average size of TiC particles existing in the sample.

Keywords: Al_2O_3; Hardness; Indentation size effect

1. Introduction

Composites of Al_2O_3–TiC consist of finely dispersed titanium carbide grains in an alumina matrix and have been used in many applications, especially as excellent cutting tools, for a long time.[1,2] In consequence, the characterization of their mechanical properties has also been an interesting subject of scientific research. During the past years, much attention has been paid to the toughness characteristics of Al_2O_3–TiC composites by noting the possible toughening effects resulting from the mismatch between the thermal and/or mechanical properties of the Al_2O_3 and TiC grains.[3,4] Up to now, however, there are few available data on the hardness characteristics of these composites, although these characteristics are of primary importance for materials considered for use as cutting tools. Therefore, the present study was designed to conduct an extensive examination on the hardness characteristics of Al_2O_3–TiC composites, with a particular emphasis on the load-dependence of the measured hardness and its effect on material evaluation based on the hardness parameter.

In general, Al_2O_3–TiC composites exhibit high hardnesses and low toughnesses. This makes it somewhat difficult to evaluate their hardness characteristics by Vickers indentation tests because, as discussed by Clinton and Morrell,[5] there may be significant errors associated with the smallness of the Vickers indentations made at lower indentation load and, while tested at higher indentation load level, microcracking due to Vickers indentation may occur and affect the hardness measurements. Thus, Knoop indentation tests, which are more insensitive to indentation-induced microcracking and yield indentations much larger than Vickers indentation in dimension, were employed in this study.

2. Experimental procedures

The materials selected for this study were Al_2O_3–30 wt.% TiC composites. The basic raw materials used for preparing the composites were a commercial Al_2O_3 powder with an average grain size of 0.5 μm and nine kinds of TiC particles whose average sizes are different from each other. The Al_2O_3 powder was mixed with one of the nine kinds of TiC particles, respectively, in proper proportion by conventional ball milling. After being dried, the mixed powders were uniaxially pressed, cold

* Corresponding author. Tel.: +86-10-62771160.
E-mail address: gong@tsinghua.edu.cn (J. Gong).

0955-2219/00/$ - see front matter
PII: S0955-2219(00)00093-5

Table 1
Average sizes of TiC particles in the test samples

Sample denotation	AC01	AC02	AC03	AC04	AC05	AC06	AC07	AC08	AC09
Size of TiC particles (μm)	0.5	1.0	1.7	2.1	3.8	4.3	5.6	6.8	8.2

isostatically pressed and then hot-pressed at 1650–1700°C and 25 MPa for 30 min.

The actual densities of the hot-pressed products were measured using the Archimedes principle and the theoretical density was calculated based on the densities of Al_2O_3 (3.987 g/mm^3) and TiC (4.911 g/mm^3) assuming a rule of mixture. The results showed that all the nine samples fabricated achieved nearly 100% of their theoretical densities. This makes it unnecessary to correlate the measured hardness with the relative density.

For microstructure characterization, the test samples were polished and then examined by scanning electron microscopy (SEM) with an image analyzer to measure the size of the TiC particles. About 200 TiC particles from each sample were measured and the results are listed in Table 1. Fig. 1 gives a typical SEM micrograph showing the polished surface of the hot-pressed product. As can be seen, the TiC particles (light phase) were well dispersed in the Al_2O_3 matrix.

The specimens used for indentation testing were cut directly from the hot-pressed products. These specimens were mounted in bakelite, ground flat using a diamond grinding wheel and then polished carefully with successively finer diamond pastes to yield a scratch-free, mirror-like surface finish suitable for indentation. The polished surface of each specimen was perpendicular to the hot-pressing direction.

Knoop indentation tests were conducted, with a low-load hardness tester (Model HK-5, Wuzhong, China) and following the procedure similar to that outlined in the ASTM standard E384 (Standard Test method for Microhardness of Materials, ASTM Designation E384, 1991. *Book of ASTM Standard*, Part 3. American Society for Testing and Materials, Philadelphia, PA), on each specimen at room temperature in the indentation load range from 1.47 to 35.77 N and at a constant dwell time of 15 s. After indentation, the length of the long diagonal of each Knoop indentation was immediately measured by optical microscopy with a magnification of 300 and an error of measurement of ±0.5 μm. The Knoop hardness number, H_K, was calculated from the measured long diagonal length for each indentation by

$$H_K = 14.229\frac{P}{d^2} \quad (1)$$

where P is the indentation load and d the long diagonal length of the Knoop indentation.

In the following discussion, the values of the long diagonal length, d, and the measured Knoop hardness, H_K, were all quoted as the average values for 10 individual indentations made at each indentation load level.

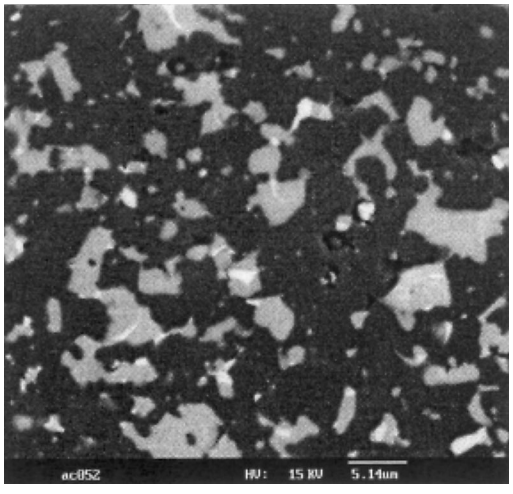

Fig. 1. SEM micrograph showing the polished surface of sample AC05. Note that the TiC particles (light phase) were well dispersed in the Al_2O_3 matrix.

3. Results and discussion

One of the obstacles in characterizing the hardness for brittle ceramics is that the measured hardness is usually load-dependent.[5–9] In general, the measured hardness decreases with increasing indentation load. Such a phenomenon has been well known as the *indentation size effect* (ISE). The ISE was also observed in the present study for the Al_2O_3–TiC composites. As an example, Fig. 2 gives the measured hardness–load curves for samples AC01, AC05 and AC09, respectively. It is clear that, for each sample, the Knoop hardness measured at the lowest load level employed, i.e. 1.47 N, is very high. With an increase in the indentation load, the measured hardness decreases gradually and then tends to an invariant level at the higher load side of the hardness–load curve. For the sake of conciseness, all the error bars corresponding to each datum point are omitted in Fig. 2. The maximum scatter, typically 7–8% of the hardness value, usually occurs at the lower load range and is reduced as the applied load increases.

As can be seen in Fig. 2, when measured at a load of 1.47 N, the Knoop hardness of sample AC01 is lower than that of sample AC09; when measured at a load of

16.17 N, however, sample AC01 exhibits a higher Knoop hardness compared with sample AC09. Similar phenomena can also be found by comparing the test results for other samples. These observations strongly suggest that the existence of the ISE makes it insufficient to quote a hardness number measured at a single load level for material characterization. A complete evaluation of the hardness characteristic for a given material needs a further knowledge of the cause of the ISE and a load-independent hardness, or true hardness.

The ISE has been traditionally described through the application of the famous Meyer's power law [5,8,9]

$$P = Ad^n \tag{2}$$

where A and n are descriptive parameters derived from the curve fitting of experimental results.

Meyer's line, which is defined by the linear relationship between $\log P$ and $\log d$ according to Eq. (2), was drawn for each sample considered, partially shown in Fig. 3, and the resultant best-fit values of the parameters, A and n are summarized in Table 2. The results showed that Eq. (2) is sufficiently suitable for the representation of the experimental data. The best-fit values of n vary between 1.79 and 1.91, depending on the materials, indicating that the composites considered in this study have no capacity for work-hardening during indentation and belong to the class of hard and brittle materials.[8]

Sargent and Page[10] have considered several "n value versus $\ln A$" relationships in an attempt to ascertain any possible microstructural effects on those power law parameters. They found that, for polycrystalline ceramics, lower n values are generally associated with higher $\ln A$ values as the grain size increases. In a study on the Vickers hardness testing for hot-pressed Si_3N_4-based ceramics, Babini et al.[8] also found that, as grain size increases, the n value increases while the A value decreases. The degree of the correlation between n and A was verified to be more evident for single crystals. By analyzing the Knoop indentation data measured on different crystallographic planes and for different crystallographic directions in two rutile-structure single crystals, TiO_2 and SnO_2, Li and Bradt[11] obtained an inverse linear relationship between n and A and this line extrapolates to $n = 2$ at $A = 0$ which was considered by Li and Bradt[12] to substantiate that Meyer's law is only applicable when an indentation size effect exists.

However, it should be pointed out that the experimental phenomena observed in the above mentioned studies seem to be of little significance for hardness characterization, because that the best-fit value of the parameter A is strongly dependent on the unit system used for recording the measured parameters P and d. For example, Fig. 4 illustrates the relationship between the Meyer's coefficient A and the Meyer's exponent n obtained in the present study. The regression analysis for deducing the best-fit values of A and n was conducted based on two different unit systems, respectively. The first unit system used is P in Newton (N) and d in millimeter (mm) and the second is P in gram (g) and d in micrometer (μm). As can be seen from Fig. 4, completely different trends of n versus A were observed in different unit systems. Similar conclusions may also be obtained by analyzing the experimental data on single crystals reported by Li and Bradt.[11] Thus, particular care should be taken when analyzing the microstructural effects on the measured hardness based on Meyer's power law.

In fact, a satisfactory explanation of the physical meanings of the parameters, A and n, included in Eq. (2) is still lacking. Little knowledge of the cause of the observed ISE may be yielded by analyzing the experimental data according to Meyer's law, although it may provide an excellent description for the experimental results. Therefore, it is necessary to progress beyond the power law description to achieve a basic understanding of the ISE.

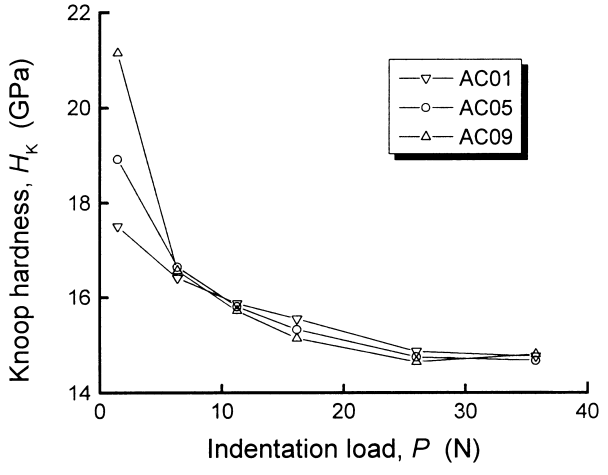

Fig. 2. Hardnesses as functions of the indentation load for samples AC01, AC05 and AC09.

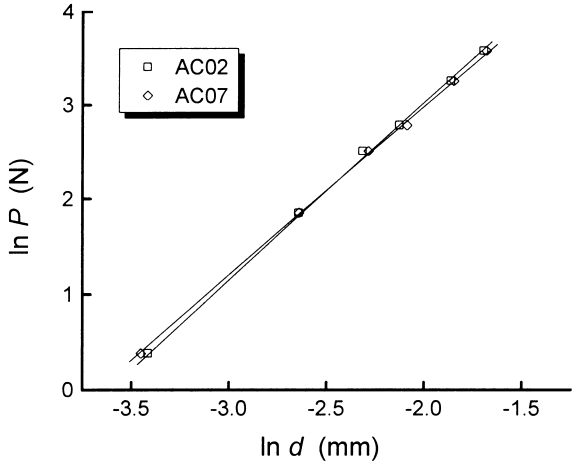

Fig. 3. Meyer's lines for samples AC02 and AC07.

Table 2
Best-fit values of Meyer's parameters, A and n, for the test samples

Sample	n	$\log A$ (N/mm^n)	Correlation factor
AC01	1.896±0.007	2.947	>0.99
AC02	1.908±0.008	2.952	>0.99
AC03	1.822±0.013	2.858	>0.99
AC04	1.824±0.014	2.881	>0.99
AC05	1.847±0.007	2.895	>0.99
AC06	1.819±0.016	2.873	>0.99
AC07	1.800±0.028	2.849	>0.99
AC08	1.826±0.018	2.874	>0.99
AC09	1.791±0.025	2.844	>0.99

Recent progress in the quantitative description of the ISE observed in ceramics may be regarded to be results of the applications of an empirical equation proposed originally by Bückle,[13]

$$P = a_0 + a_1 d + a_2 d^2 + \cdots a_n d^n \tag{3}$$

where $a_i (i = 0, 1, ..., n)$ are adjustable constants. It was usually suggested that the a_0-term in Eq. (3) corresponds to a load threshold for an indenter to make a permanent indentation and has such a low magnitude that it can be ignored in most situations.[9] Furthermore, a good fit of experimental data was often obtained utilizing only two of the power series terms.[11,14] This results in an expression for correlating the indentation load, P, to the resultant indentation size, d,

$$P = a_1 d + a_2 d^2 \tag{4}$$

There have been two different approaches for discussing the physical meaning of Eq. (4), one being the energy-balance model which was established by Fröhlich et al.[14] and the other being the "proportional specimen resistance (PSR)" model developed by Li and Bradt.[11] One of the main conclusions yielded from both approaches is that, during an indentation process, only a part of the total indentation load is used for the volume deformation or the permanent deformation and, as a result, the true hardness, H_T, should be calculated based on the effective test load, P_{eff}, rather than the total test load, P, i.e.

$$H_T = \kappa \frac{P_{eff}}{d^2} = \kappa \left(\frac{P - a_1 d}{d^2} \right) = \kappa a_2 \tag{5}$$

where κ is a constant dependent only on the indenter geometry. For Knoop indenter, $\kappa = 14.229$.

Although a self-consistent explanation was yielded when analyzing the ISE observed in some materials with Eq. (4), [6,7,11,14], it should be pointed out that Eq. (4) is insufficient for describing the experimental data measured in a relatively wider range of indentation load. For example, Eq. (4) predicts that there is a linear relationship between P/d and d; but a significant non-linearity behavior has been observed when plotting the experimental data measured with a series of Si_3N_4-based ceramics on the $P/d - d$ scale.[15,16] This fact has been further confirmed in a more extensive study[17] concerning the ISE in some typical ceramics and it was suggested that, when examining the ISE in brittle materials, treating a_0-term in Eq. (3) to be zero seems to be unreasonable and the indentation load, P, should be related to the resultant indentation size, d, by

$$P = a_0 + a_1 d + a_2 d^2 \tag{6}$$

Applications of Eq. (6) to the experimental results for samples AC03 and AC08 are shown in Fig. 5. Correlations for these plots, as well as the plots for other samples tested in the present study, are very high, $r^2 > 0.99$.

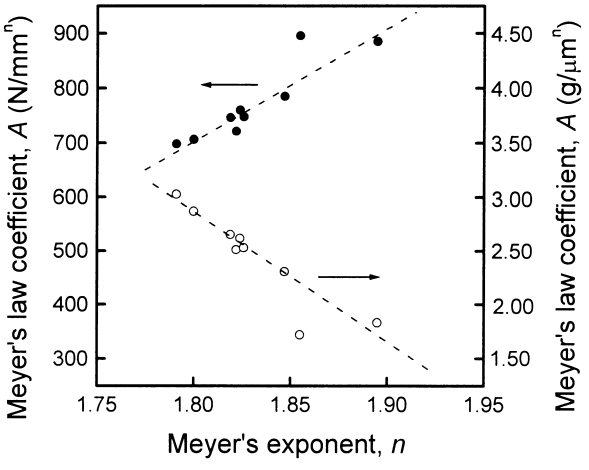

Fig. 4. Variation of Meyer's law coefficient A with Meyer's exponent n. Note that completely different trends are observed when different unit systems were used for recording the experimental data.

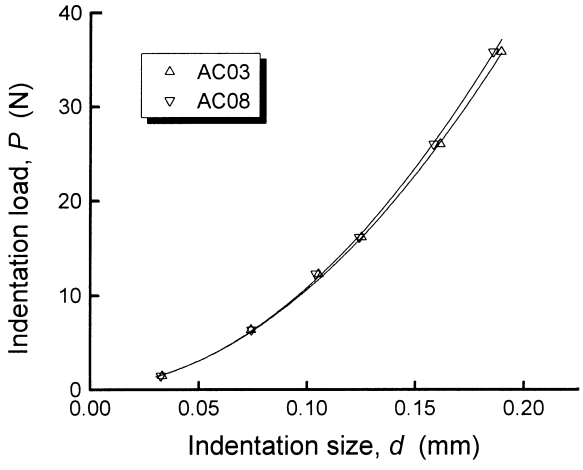

Fig. 5. Applications of Bückle's empirical equation to the experimental data for samples AC03 and AC08.

Table 3 summarizes the best-fit values of all the three parameters, a_0, a_1 and a_2, for all the nine samples considered.

The physical meaning of Eq. (6) has been discussed based on the PSR model.[15–17] Starting from the analysis by Li and Bradt,[11] the parameter a_0 in Eq. (6) has been suggested to be a measure of the effect of the machining-introduced plastically deformed surface on the hardness measurement. In other words, a_0 may be related directly to the magnitude of the machining-introduced residual surface stresses in the specimen. On the other hand, according to the analysis of Li and Bradt,[11] the parameters a_1 and a_2 can be related to the elastic and the plastic properties of the test material, respectively. Note that the material parameter E/H (where E is the elastic modulus) is a measure of the magnitude of the indentation residual stress resulting from the mismatch between the plastic zone beneath the indentation and the surrounding elastic matrix.[18] Analogously, the a_1/a_2 ratio may be treated approximately as a measure of the residual surface stresses due to machining. Fig. 6 shows the determined a_0-value as a function of the a_1/a_2-ratio. The correlation between these two parameters is evident, giving a further support for the previous discussion[17] on the physical meaning of Eq. (6).

Table 3
Best-fit values of the parameters included in Eq. (6) for the test samples

Sample	a_0 (N)	a_1 (N/mm)	a_2 (N/mm^2)	Correlation factor
AC01	−0.441	23.72	919.4±25.2	>0.99
AC02	−0.594	26.56	910.2±25.3	>0.99
AC03	0.088	14.13	912.3±32.9	>0.99
AC04	0.039	17.31	943.5±47.0	>0.99
AC05	0.143	18.91	930.4±24.8	>0.99
AC06	0.162	11.93	968.5±36.4	>0.99
AC07	0.244	7.98	979.6±16.5	>0.99
AC08	0.218	8.78	976.4±33.8	>0.99
AC09	0.369	6.73	986.5±45.7	>0.99

A further comment should be made on the best-fit value of a_0 listed in Table 3. In a previous study[17] on the ISE in several typical ceramics, the a_0-values were determined to be negative for all the test materials. Considering that the machining-introduced residual surface stresses are compressive in general, those negative a_0-values were suggested to be reasonable.[17] The a_0-values determined in the present study vary between −0.6 and +0.4, indicating that the residual surface stresses may be tensile in some samples and compressive in others. This phenomenon can be understood easily by noting the fact that the machining-introduced residual stresses are compressive near the surface and tensile underneath.[19] As mentioned above, Al_2O_3–TiC composites usually exhibit high hardness. This would make it more difficult to plastically deform the Al_2O_3–TiC composites. As consequence, the machining-introduced residually stressed surface layer in the test specimen is generally thinner compared with most of the materials used in Ref. 17. After being carefully polished, one can expect that, for some samples, the surface layer in a state of compression may be removed and, as a result, the experimentally estimated a_0-values for these samples may turn to positive.

Having concluded that Eq. (6) is suitable for describing the ISE observed in the present Al_2O_3–TiC composites, it is of interest to estimate the true hardness for each sample from the parameter a_2 in Eq. (6). Similar to the analysis of Li and Bradt,[11] the effective test load, P_{eff}, used for the permanent deformation during an indentation event may now be expressed as

$$P_{\text{eff}} = P - (a_0 + a_1 d) \tag{7}$$

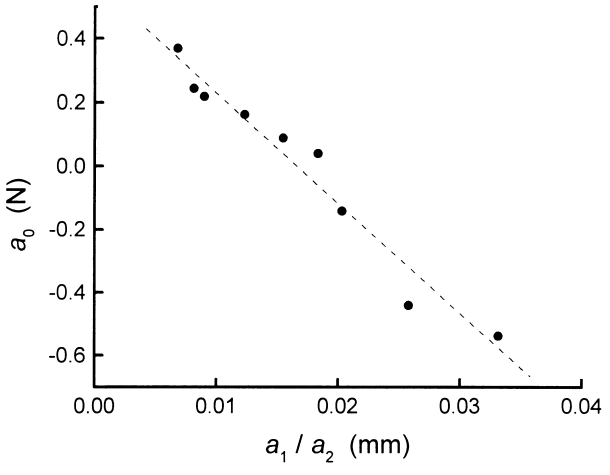

Fig. 6. Variation of a_0 with the a_1/a_2-ratio.

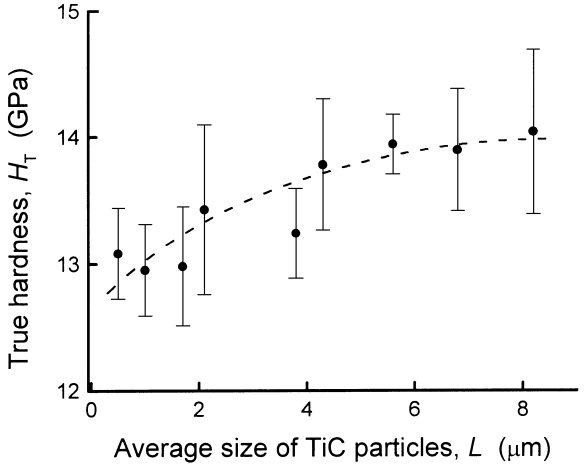

Fig. 7. True hardness of Al_2O_3–30 wt.% TiC composites as a function of the average size of TiC particles in the test sample.

Thus, the true hardness, H_T, may be calculated by

$$H_T = \kappa \frac{P_{eff}}{d^2} = \kappa\left(\frac{P - a_0 - a_1 d}{d^2}\right) = \kappa a_2 \quad (8)$$

The true hardness for each sample tested was calculated with Eq. (8) and $\kappa = 14.229$ using the best-fit values of a_2 listed in Table 3. The result is shown in Fig. 7 as a function of the average size of TiC particles in the test sample. It is seen that, as the average size of TiC particles increases, the true hardness of Al_2O_3–30 wt.% TiC composite increases slightly.

4. Conclusions

The load-dependence of Knoop hardness of Al_2O_3–30 wt.% TiC composites was examined in this study.

The following conclusions were deduced:

a. In the test load range, from 1.47 to 35.77 N, all the samples exhibit a significant indentation size effect, making it impossible to conduct a comparison between materials based on a hardness number measured at only a single test load level.

b. The classical Meyer's power law may give a good fit for the measured indentation data. The best-fit value of the Meyer's law coefficient A strongly depends on the unit system used for recording the experimental data. Little useful information may be yielded from the analysis based on Meyer's law.

c. The empirical equation, Eq. (6), proposed originally by Bückle was proven to be suitable for describing the observed ISE. True hardness number may be deduced from this equation. It was shown that the deduced true hardness increases slightly with the average size of TiC particles existing in the test sample.

References

1. Masuda, M., Sato, T., Kori, T. and Chujo, Y., Cutting performance and wear mechanism of alumina-based ceramic tools when machining austempered ductile iron. *Wear*, 1992, **174**, 147–153.
2. Takahashi, T., Development of fine and high-strength Al_2O_3 based ceramics. *J. Jpn. Soc. Powder & Powder Metall*, 1998, **45**, 496–506.
3. Furukawa, M., Nakano, O. and Takashima, Y., Fracture toughness of Al_2O_3–TiC ceramics. *Int. J. Refrac. & Hard Metals*, 1988, **7**, 37–40.
4. Tamari, N., Tanaka, T., Kondoh, I., Tezuka, K. and Yamamoto, T., Mechanical properties and cutting performance of titanium carbide whisker/alumina composites. *J. Ceram. Soc. Jpn*, 1996, **104**, 439–444.
5. Clinton, D. J. and Morrell, R., Hardness testing of ceramic materials. *Mater. Chem. Phys*, 1987, **17**, 461–473.
6. Micheles, B. D. and Frischat, G. H., Microhardness of chalcogenide glasses of the system Se–Ge–As. *J. Mater. Sci.*, 1982, **17**, 329–334.
7. Hirao, K. and Tomozawa, M., Microhardness of SiO_2 glass in various environments. *J. Am. Ceram. Soc.*, 1987, **70**, 497–502.
8. Babini, G. N., Bellosi, A. and Galassi, C., Characterization of hot-pressed silicon nitride based materials by microhardness measurements. *J. Mater. Sci.*, 1987, **22**, 1687–1693.
9. Quinn, J. B. and Quinn, G. D., Indentation brittle of ceramics: a fresh approach. *J. Mater. Sci.*, 1997, **32**, 4331–4346.
10. Sargent, P. M. and Page, T. F., The influence on the microhardness of ceramic materials. *Proc. Brit. Ceram. Soc.*, 1978, **26**, 209–224.
11. Li, H. and Bradt, R. C., The microhardness indentation load/size effect in rutile and cassiterite single crystals. *J. Mater. Sci.*, 1993, **28**, 917–926.
12. Li, H. and Bradt, R. C., Knoop microhardness anisotropy of single crystal cassiterite (SnO_2). *J. Am. Ceram. Soc.*, 1991, **74**, 1053–1060.
13. Bückle, H., *Mikrohärteprüfung*. Berliner Union Verlag, Stuttgart, 1965.
14. Fröhlich, F., Grau, P. and Wrellmann, W., Performance and analysis of recording microhardness tests. *Phys. Status Solidi*, 1977, **42**, 79–89.
15. Gong, J., Wu, J. and Guan, Z., Description of the indentation size effect in hot-pressed silicon-nitride-based ceramics. *J. Mater. Sci. Lett.*, 1998, **17**, 473–475.
16. Gong, J., Wu, J. and Guan, Z., Load dependence of the apparent hardness of silicon nitride ceramics in a wider range of loads. *Mater. Lett.*, 1998, **35**, 58–61.
17. Gong, J., Wu, J. and Guan, Z., Examination of the indentation size effect in low-load Vickers hardness testing of ceramics. *J. Eur. Ceram. Soc.*, 1999, **19**, 2625–2631.
18. Lawn, B. R., Evans, A. G. and Marshall, D. B., Elastic/plastic indentation damage in ceramics: the median/radial crack system. *J. Am. Ceram. Soc.*, 1980, **63**, 574–581.
19. Samuel, R., Chandrasekar, S., Farris, T. N. and Licht, R. H., Effect of residual stresses on the fracture strength of ground ceramics. *J. Am. Ceram. Soc.*, 1989, **72**, 1960–1966.